Optica Applicata, Vol. LII, No. 1, 2022
DOI: 10.37190/oa220107

Active control of terahertz wave assisted by dielectric loaded plasmonic waveguide

Huaiqing Liu[1], Mengya Yang[1], Xue He[1], Youchao Jiang[2], Xiancun Zhou[1], Maosheng Fu[1*]

[1]College of Electronic and Information Engineering, West Anhui University, Luan 237012, China

[2]Key Lab of All Optical Network & Advanced Telecommunication Network of EMC, Beijing Jiaotong University, Beijing 100044, China

[*]Corresponding author: fums@wxc.edu.cn

We propose and numerically investigate a directional coupler which consists of two dielectric loaded InSb based terahertz (THz) plasmonic waveguides. Owing to the permittivitly tunable property of InSb, the coupling strength between the two dielectric loaded plasmonic waveguides is affected by temperature, so the maximum power coupled from the input waveguide to the cross-waveguide and the correspondingly coupling length could be effectively tailored by altering temperature. Under different temperatures, this directional coupler could act as a thermally controlled terahertz wave switch or a 3-dB terahertz splitter around the frequency of 1.17 THz. This ultracompact and thermally controlled plasmonic directional coupler may find potential important applications in the highly integrated photonic circuits for terahertz system and technologies.

Keywords: terahertz, plasmonic, coupling, switch, splitter.

1. Introduction

Terahertz technology has drawn extensive attention in relation to various application fields such as biological science, medical imaging, security and space science [1–5]. Intensive studies fueled by emerging applications of THz frequency are now focusing on developing various functional devices such as emitters, modulators, filters, detectors, and absorbers in efforts to realize THz systems with better performance and new functions [6–9]. Thus, it is necessary to find approaches to active control of THz wave with external elements such as voltage, magnetic field, and temperature.

On the other hand, integrated photonic circuits have drawn extensive research interests aiming at realizing high-speed, large-capacity and low-power optical communication system. Surface plasmon polaritons (SPPs) are electromagnetic waves propagating along dielectric–metal interfaces and can be confined by metallic nanostructures beyond

the diffraction limit [10], which could benefit the development of highly integrated photonic circuits. And due to the development of the technologies that made the fabrication of nanostructures possible as well as the increasing demand for computer chips, plasmon-polaritons based devices, such as plasmonic waveguide, filters, absorbers, and beam shaping [11–17], have attracted numerous interests of researchers over the past decade. In order to realize a highly integrated THz system, there is an urgent need to find a material that can support THz SPP mode. Graphene seems a good candidate for supporting THz SPP wave, and graphene has been introduced to construct terahertz plasmonic devices due to its exceptional properties, such as optical transparency, flexibility, and tunable structures were several mm. However, the structures based on graphene are demanding in terms of costs and complexity, and the thickness of graphene is just about 0.34 nm so that it is fragile. Another alternative promising material for terahertz plasmonic device is moderately doped semiconductor, which can be readily fabricated using conventional micro-fabrication techniques. Some semiconductors have a permittivity at THz region close to that of metal at optical range. Such as InSb, whose permittivity can be modified by varying temperature, has been proposed for designing THz plasmonic devices [18–21], besides, it is easy to obtain and the manufacturing process is simple, active control of THz wave utilizing InSb based plasmonic waveguide by tuning temperature seems interesting and promising.

In this paper, we propose a dielectric-loaded InSb plasmonic waveguide (DLIPW) working at THz region, which is similar to the dielectric-loaded metal plasmon waveguide in a near-infrared range. Owing to the permittivity tunable property of InSb, the coupling strength between the two dielectric loaded plasmonic waveguide is affected by temperature, so the maximum power coupled from the input waveguide to the cross -waveguide and the corresponding coupling length could be effectively tailored by varying temperature. At different temperatures, this directional coupler could act as a thermal controlled terahertz wave switch or a terahertz splitter at the frequency of 1.17 THz. This ultracompact and thermal controlled plasmonic directional coupler may find important applications in the highly integrated photonic circuits for THz devices and technologies.

2. Structure design and principle

The schematic diagram of our dielectric loaded THz plasmonic waveguide is shown in Fig. 1. The whole size of the substrate is 1400×900 mm^2, the inset is the *xy* plane side view of our structure. Two parallel identical straight DLIPWs with edge-to-edge separation d constitute the coupling region. And the coupling regions with a length of L are connected to the output waveguide (Ps and Pc) by a straight and bend waveguide, respectively. The width and height of the SiO_2 rectangular waveguide are denoted as w and h. The thickness of the InSb layer and the Si substrate are defined as t_1 and t_2. The incident THz wave is illuminated from one port as depicted in Fig. 1, when neglecting the waveguide loss, the incident power could be shared by the two output port Ps and Pc. Due to the fact that the permittivity of InSb could be tuned by varying temper-

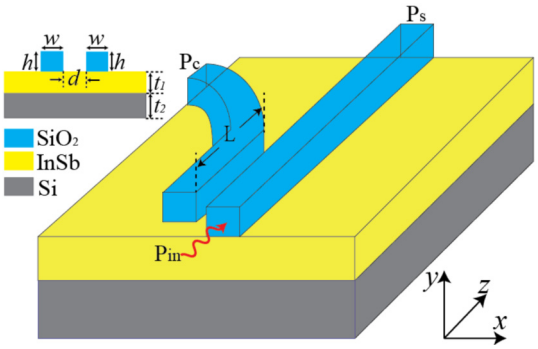

Fig. 1. Schematic diagram of THz plasmonic dielectric loaded waveguide, the inset shows the *xy*-plane side view of this waveguide.

ature, thus, by properly choosing temperature, the output power in the two output port could be activity controlled. Inspired by this mechanism, we think that the coupling between two parallel straight DLIPWs could be dynamically controlled, leading to thermal tunable directional coupler (DC). Assisted by this DC, active THz plasmonic devices such as THz switch and splitter could be achieved. InSb is a semiconductor that can support THz SPP wave, the permittivity of InSb can be approximately given by the simple Drude model approximation [22]

$$\varepsilon(\omega) = \varepsilon_\infty - \frac{\omega_p^2}{\omega^2 + i\gamma\omega} \tag{1}$$

where, ε_∞ denotes the high-frequency permittivity, ω is angular frequency, and γ is the damping constant. The plasma frequency $\omega_p = \sqrt{Ne^2/\varepsilon_0 m^*}$ depends on the intrinsic carrier density N, the electronic charge e, the vacuum permittivity ε_0, and the effective mass m^* of free carriers. The intrinsic carrier density N (in m^{-3}) of InSb can be expressed as [23]

$$N = 5.76 \times 10^{20}\, T^{1.5} \exp(-0.26/2k_B T) \tag{2}$$

where, k_B is the Boltzmann constant and T is the temperature in kelvin. It should be noted that the damping constant γ of InSb is proportional to the electron mobility μ as $\gamma = em^*/\mu$, which in turn depends on the temperature. Thus, while changing the temperature, γ will change as well and then it will influence the absorption property of InSb. However, when the temperature ranges from 160 to 350 K within the frequency regime from 0.1 to 2.2 THz, the electron mobility μ changes slightly. Consequently, the damping constant can be seen as a constant, which is consistent with the experimental results in [24, 25]. For InSb, $\varepsilon_\infty = 15.6$, $m^* = 0.015m_e$ (m_e is the mass of electron), and $\gamma = 5 \times 10^{10}$ Hz [26–28].

Here, we first consider a single SiO_2 waveguide placed on the InSb semiconductor, the geometry parameters are set as $w = h = 100$ μm, $t_1 = 400$ μm, and $t_2 = 600$ μm. In

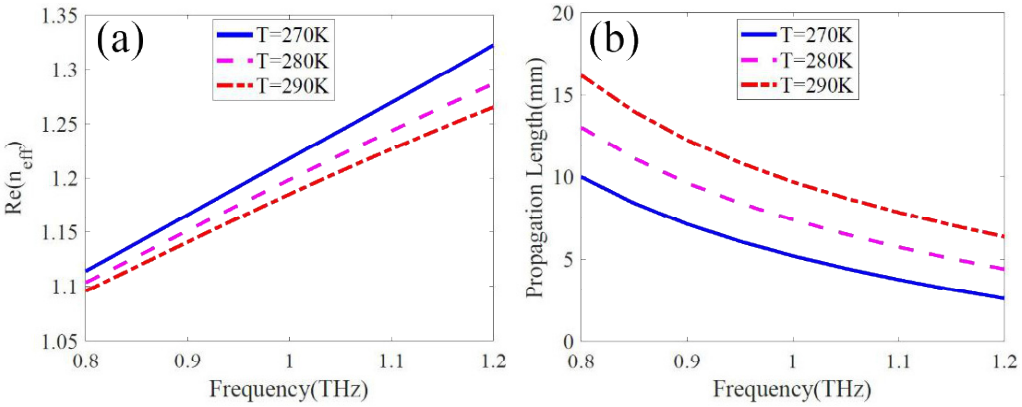

Fig. 2. (**a**) Real part of the effective mode index as a function of the frequency for different temperatures. (**b**) The propagation length of the SPP mode in this waveguide as a function of frequency for various temperatures.

this paper, all numerical calculations have been performed by using the commercial FEM software COMSOL Multiphysics. The simulated effective refractive index and the propagation length as a function of frequency for various temperature are shown in Figs. 2**a** and 2**b**, respectively. Seeing from Fig. 2**a**, it shows that the effective refractive index of the SPP mode in this THz plasmonic waveguide gets smaller when increasing temperature. It worth mentioning that the loss of this waveguide is determined by the imaginary part of the effective refractive index of the SPP mode in the waveguide, and it refers to the propagation length that is defined as the length over which the power carried by the wave decays to $1/e$ of its initial value $L_{spp} = \lambda_0/[4\pi\,\mathrm{Im}(n_{eff})]$ [29], the corresponding propagation length is shown in Fig. 2**b**, it can be seen that the SPP wave can propagate tens of millimeters for lower frequency and several millimeters for higher frequency. We can also see that the propagation length gets longer while increasing temperature, which means this waveguide has lower loss for high temperature system.

Due to the fact that the effective index of the SPP mode supported by the InSb-dielectric surface, so by varying temperature, the coupling effect between the two DLIPWs could be actively controlled. Transmission characteristics of the DC could be analyzed by the well-established coupled-mode theory (CMT), in which electromagnetic field distribution in the DC can be expressed as the superposition of the symmetrical and anti-symmetrical supermodes. For a fixed coupling length, the power coupled from one waveguide to the other is determined by the effective mode index of symmetrical $(n_s = n_s' - in_s'')$ and anti-symmetrical $(n_a = n_a' - in_a'')$ supermodes.

Numerical modeling technique results presented in this paper are based on the finite -difference time-domain (FDTD) method. In the two dimension (2D) simulations, the width and thickness of the DLIPW are both 100 μm, which ensures single mode operation from the wavelength of 0.8 to 1.2 THz. The distance between the two SiO_2 waveguides is chosen as 150 μm. The refractive index of SiO_2 and Si are assumed as 1.45 and 3.48, respectively. The temperature is assumed as room temperature 290 K.

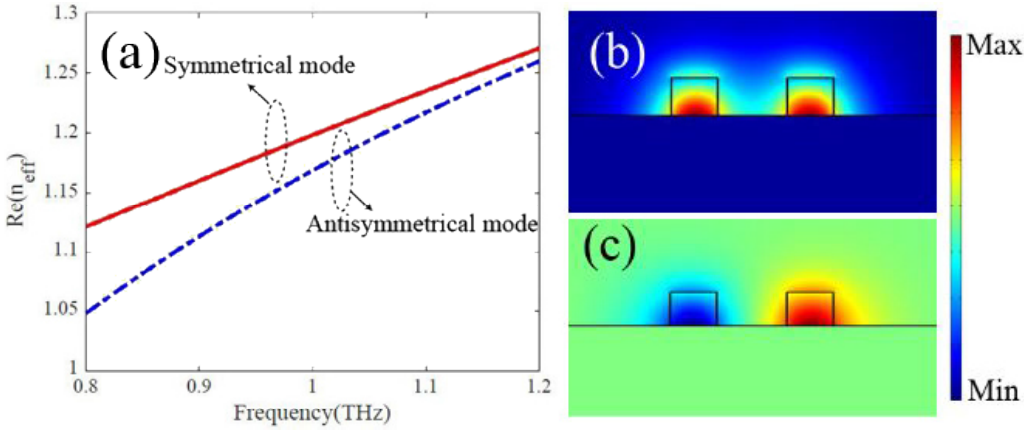

Fig. 3. (**a**) Real part of the effective mode index of symmetrical and anti-symmetrical modes as a function of the frequency of the incident source. (**b**) and (**c**) show that the *y*-direction electric filed component H_y of the mode corresponds to symmetrical mode and anti-symmetrical mode at 1 THz, respectively.

The mode dispersion relations (real part of the effective mode index) of the supermodes for different width of SiO_2 layers are shown in Fig. 3.

3. Results and discussions

The permittivity of InSb is dependent on temperature, so the effective index of the SPP mode in the InSb-medium surface depends on both the width of the insulator slit and the temperature according to Eq. (3). To simplify the model, we choose the insulator as air ($\varepsilon_d = 1$) at first. The effective index in the InSb–air surface with 1 THz incident source calculated from Comsol Multiphysics based on the finite element method (FEM) is plotted in Fig. 2. Seeing from Fig. 2, it is evident that the effective refractive index of the SPP mode in our structure changes dramatically when varying the width of the air slit. In addition, for a fixed air slit width, the effective index depends on the temperature. Therefore, controlling the plasmonic THz planar lens by altering temperature seems possible and interesting.

The coupling efficiency plays an important role in a coupled waveguide system. Here, the coupling efficiency between the two SiO_2 waveguides is estimated by calculating the vector overlap integral in the following form [30]:

$$h = \frac{\left|\iint_A \mathbf{E}_1 \times \mathbf{H}_2 \cdot \hat{\mathbf{z}}\,\mathrm{d}x\,\mathrm{d}y\right| \left|\iint_A \mathbf{E}_2 \times \mathbf{H}_1 \cdot \hat{\mathbf{z}}\,\mathrm{d}x\,\mathrm{d}y\right|}{\left|\iint_A \mathbf{E}_1 \times \mathbf{H}_1 \cdot \hat{\mathbf{z}}\,\mathrm{d}x\,\mathrm{d}y\right| \left|\iint_A \mathbf{E}_2 \times \mathbf{H}_2 \cdot \hat{\mathbf{z}}\,\mathrm{d}x\,\mathrm{d}y\right|} \tag{3}$$

According to the above equation, the simulated coupling efficiency between the two SiO_2 waveguides as a function of frequency for various coupling distances is shown in Fig. 4. Obviously, the coupling efficiency is inversely related to the distance between

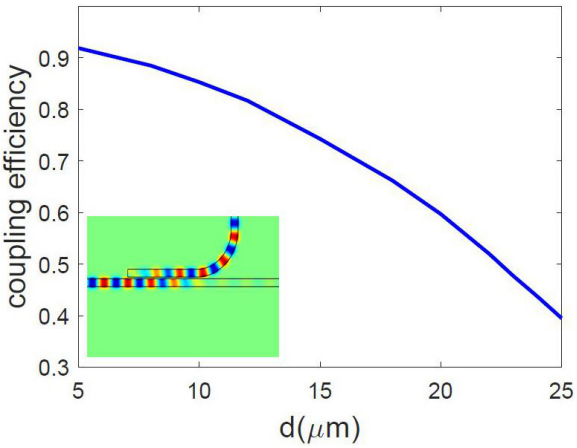

Fig. 4. The coupling efficiency as a function of the coupling distance between the two SiO_2 waveguides, the temperature is kept as 270 K. The inset shows an example of the maximum power coupled from the straight SiO_2 waveguide to the bend SiO_2 waveguide at a special coupling condition; the geometric parameters are set as $w = h = 100$ μm, $L = 500$ μm, $t_1 = 400$ μm, $t_2 = 600$ μm and $d = 10$ μm.

the two SiO_2 waveguides. Thus a smaller value of d is better for achieving high coupling efficiency. It is worth noting that the coupling length L is quite important in the coupling process between the two waveguides. In this paper we choose $L = 500$ μm to make sure that the two waveguides can be fully coupled. And the inset shows the magnetic field along the y direction of our coupler with $d = 10$ μm as a special frequency corresponds to the condition of maximal power coupled from one waveguide to the other. It shows that at this condition nearly all of the incident power has been transferred from the straight waveguide to the bend one. So it is possible to manipulate THz wave on this type dielectric loaded waveguide by properly choosing geometric parameters and the temperature of the surroundings. It should be noted that the distance between the two waveguide plays an important role in the structure, thus the smaller the separation distance d, the stronger the coupling strength, but too close spacing will increase manufacturing process difficulties. So a reasonable d is crucial in our structure.

Here, aiming to achieve a high efficiency coupler while keeping low crosstalk between the two dielectric waveguides, the distance between the two dielectric loaded waveguides is set to be 10 μm, and the other parameters are the same as in Fig. 4. The simulated transmission of the two output ports and the side view of the magnetic field component along z direction (H_y) at several frequencies are displayed in Fig. 5. Seeing from Fig. 5**a**, we can notice that the output power of the straight SiO_2 waveguide (Ps) decreases when increasing the frequency of the incident THz wave, while the output power of the bend one (Pc) increases when increasing the frequency of the incident wave. Figures 5**b**–5**d** shows the magnetic field along z direction at three different frequencies such 0.4, 1.15 and 1.38 THz, respectively. Apparently, at the frequency of 0.4 THz, there is little energy coupled to the bend waveguide and most power is transmitted to the Ps. When the frequency of the incident wave increases, the cou-

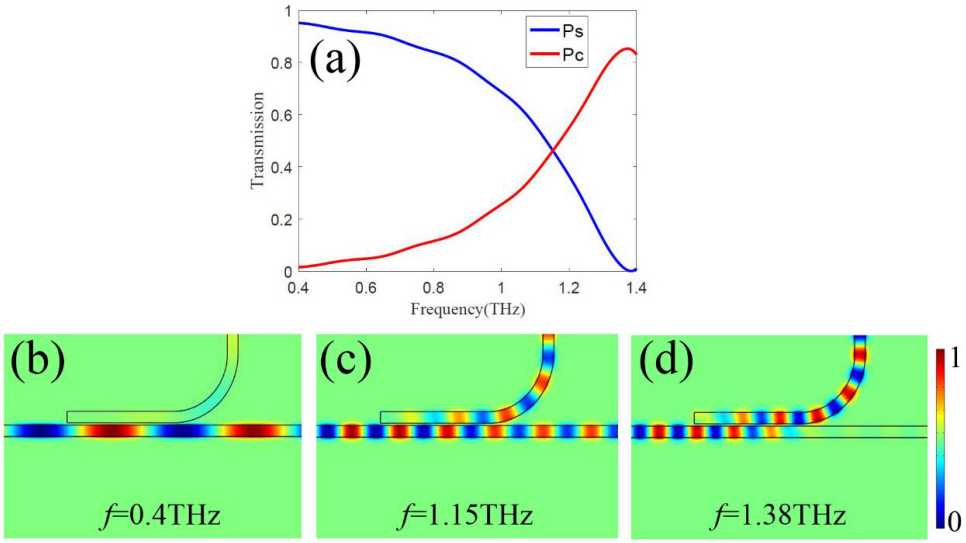

Fig. 5. (**a**) The transmission of the two output ports as a function of frequency. (**b**)–(**d**) shows the side view of the *y*-direction magnetic field component H_y at the frequency of 0.4, 1.15, and 1.38 THz, respectively.

pling condition for the maximal power coupled from the straight waveguide to the bend one is satisfied, leading to most power coupled from Ps to Pc at 1.38 THz. Thus the input power can switch from the straight SiO_2 waveguide to the bend one when increasing the frequency of the incident source. Meanwhile, we can see that the two transmission lines have an intersection at the frequency close to 1.15 THz, and the corresponding H_y is shown in Fig. 5**c**. It is obvious that the power is nearly transmitted equally to the two output ports, so this dielectric loaded waveguide can also act as a THz wave splitter if the parameters are properly designed. It is worth noting that at the frequency of 1.38 THz, the value of the Pc is smaller than the value of Ps at 0.4 THz. This is due to the coupling loss and larger propagating loss when increasing the frequency of the incident THz wave.

As the permittivity of InSb can be controlled by varying temperature, so we believe that the THz wave in this InSb based dielectric plasmonic can be tailored by altering temperature. Here, in order to investigate the dependence of the function of our structure on temperature, we chose the geometric parameters to be the same as Fig. 5, and the working frequency is set to be 1.17 THz. At first, the temperature is assumed as 260 K, which is lower than room temperature, the simulated transmission of the two output ports is shown in Fig. 6**a**. Seeing from Fig. 6**a**, we found that at the frequency of 1.17 THz, Ps is close to zero and Pc reaches its maximum, which means that the power can only be transmitted to the bend coupling waveguide. It is consistent with Fig. 6**d**, which shows the magnetic field along the *y* direction (H_y), when nearly all of the input power is coupled to the bend waveguide; this phenomenon corresponds to the optimal coupling state. We investigate the thermal property of our structure by observing the transmission property of the two output ports when varying temperature. The results for

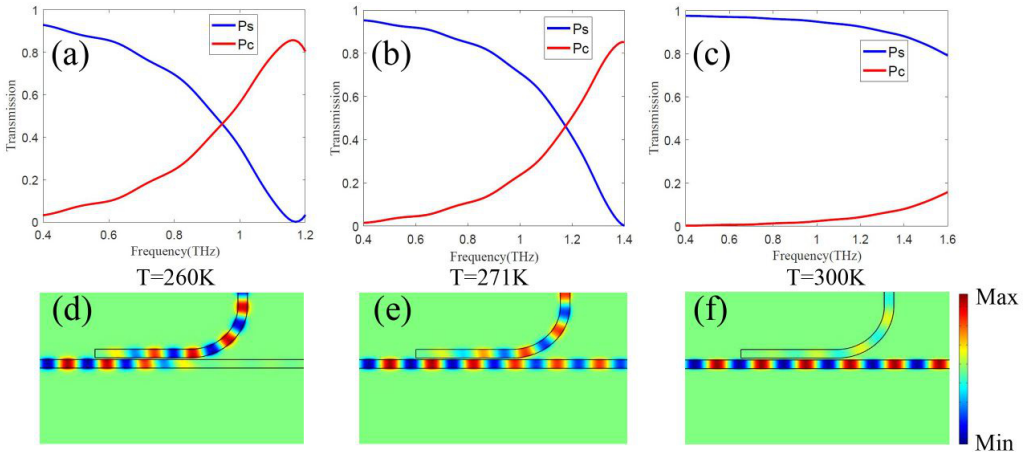

Fig. 6. (**a**) The transmission property of the two output ports for various temperature, the geometric parameters are the same as Fig. 5. (**b**)–(**d**) shows the side view of the *y*-direction magnetic field component H_y for the frequency of 1.17 THz with $T = 260$ K, $T = 271$ K and $T = 300$ K, respectively.

$T = 271$ K and $T = 300$ K are displayed in Figs. 6**b** and 6**c**, respectively. We can see that when $T = 271$ K, the two transmission lines for Ps and Pc intersect near 1.17 THz, and seeing from Fig. 6**e**, it is obvious that the power transmitted to the two output ports is nearly equal; so at this condition this structure can act as a THz wave splitter. However, when we further increase the temperature to 300 K, the corresponding results at 1.17 THz are shown in Figs. 6**c** and 6**f**. Obviously, at this condition, the power can hardly be coupled from the straight waveguide to the bend one, so most of the input power is transmitted to the straight output port. In other words, as the temperature increases, the coupled power in the bend waveguide can be released and come back to the original transmission route. So we can see that at the frequency of 1.17 THz, our structure has different function when altering the temperature. When $T = 271$ K, our structure can be regarded as a THz splitter. While, when the temperature changes from 300 to 260 K, the power can be switched from the straight to the bend one. At this condition, our structure can be regarded as a temperature-controled THz switch. Thus, one can manipulate THz wave in our structure by controlling temperature without needing to alter the geometric parameters. And our structure is prior to graphene in terms of simpler fabrication procedure and cheaper material, so our structure may find potential important applications in THz plasmonic system and devices.

Last but not least, for practical applications, the fabrication process of our structure should also be taken into account. At first, we can place the molten semiconductor InSb on the silicon substrate, and then we can use the electron beam lithography (EBL) technology to obtain a cubic Si-InSb substrate. At last we can lay the molten cuboid-shaped silica waveguide on the Si-InSb substrate, and after the air drying process, we can obtain the model as shown in Fig. 1.

4. Conclusion

In this paper, we proposed and numerically investigated a dielectric-loaded InSb based plasmonic waveguide, which can support THz SPP wave. The dispersion relationship of this waveguide is analyzed and discussed, and it can support two kinds of THz SPP wave, including symmetrical mode and anti-symmetrical mode. The simulated results reveal that the power can be selectively transmitted to the output port at different frequency. Due to the fact of the permittivity tunable property of InSb, the maximum power coupled from the straight SiO_2 waveguide to the bend one can be effectively tailored by varying temperature. Under different temperature, this directional coupler could act as a thermal controlled terahertz wave switch or a terahertz splitter at the frequency of 1.17 THz. This ultracompact and thermally controlled plasmonic directional coupler may be beneficial for the development of the highly integrated photonic circuits for THz devices and technologies.

Acknowledgement
The project was funded by the State Key Laboratory of Advanced Optical Communication Systems Networks, China (Grant No. 2020GZKF006) and the National Science Fund of China (Grant No. 61572366) and the Zhejiang Natural Science Foundation (Grant No. LQ19F050002). This work was also funded by the Ningbo Natural Science Foundation (Grant No. 2018A610089).

References

[1] Tonouchi M., *Cutting-edge terahertz technology*, Nature Photonics **1**(2), 2007, pp. 97–105, DOI: 10.1038/nphoton.2007.3.

[2] Ferguson B., Zhang X.C., *Materials for terahertz science and technology*, Nature Materials **1**(1), 2002, pp. 26–33, DOI: 10.1038/nmat708.

[3] Fischer B.M., Hoffmann M., Helm H., Wilk R., Rutz F., Kleine-Ostmann T., Koch M., Jepsen P.U., *Terahertz time-domain spectroscopy and imaging of artificial RNA*, Optics Express **13**(14), 2005, pp. 5205–5215, DOI: 10.1364/OPEX.13.005205.

[4] Auton G., But D.B., Zhang J., Hill E., Coquillat D., Consejo C., Nouvel P., Knap W., Varani L., Teppe F., Torres J., Song A., *Terahertz detection and imaging using graphene ballistic rectifiers*, Nano Letters **17**(11), 2017, pp. 7015–7020, DOI: 10.1021/acs.nanolett.7b03625.

[5] Kaltenecker K., Zhou B., Tybussek K.-H., Engelbrecht S., Lehmann R., Walker S., Jepsen P.U., Fischer B.M., *Ultra-broadband THz spectroscopy for sensing and identification for security applications*, [In] *2018 43rd International Conference on Infrared, Millimeter, and Terahertz Waves (IRMMW-THz)*, 2018, DOI: 10.1109/IRMMW-THz.2018.8510500.

[6] Diem M., Koschny T., Soukoulis C.M., *Wide-angle perfect absorber/thermal emitter in the terahertz regime*, Physical Review B **79**(3), 2009, article 033101, DOI: 10.1103/PhysRevB.79.033101.

[7] Kleine-Ostmann T., Dawson P., Pierz K., Hein G., Koch M., *Room-temperature operation of an electrically driven terahertz modulator*, Applied Physics Letters **84**(18), 2004, p. 3555, DOI: 10.1063/1.1723689.

[8] Khan M.J., Chen J.C., Kaushik S., *Optical detection of terahertz radiation by using nonlinear parametric upconversion*, Optics Letters **32**(22), 2007, pp. 3248–3250, DOI: 10.1364/OL.32.003248.

[9] Wang B.-X., Wang L.-L., Wang G.-Z., Huang W.-Q., Li X.-F., Zhai X., *Theoretical investigation of broadband and wide-angle terahertz metamaterial absorber*, IEEE Photonics Technology Letters **26**(2), 2014, pp. 111–114, DOI: 10.1109/LPT.2013.2289299.

[10] BARNES W.L., DEREUX A., EBBESEN T.W., *Surface plasmon subwavelength optics*, Nature **424**, 2003, pp. 824–830, DOI: 10.1038/nature01937.
[11] WANG B.-X., WANG L.-L., WANG G.-Z., HUANG W.-Q., LI X.-F., ZHAI X., *Frequency continuous tunable terahertz metamaterial absorber*, Journal of Lightwave Technology **32**(6), 2014, pp. 1183–1189, DOI: 10.1109/JLT.2014.2300094.
[12] GAN F., SUN C., LI H., GONG Q., CHEN J., *On-chip polarization splitter based on a multimode plasmonic waveguide*, Photonics Research **6**(1), 2018, pp. 47–53, DOI: 10.1364/PRJ.6.000047.
[13] ZHENG K., SONG J., QU J., *Hybrid low-permittivity slot-rib plasmonic waveguide based on monolayer two dimensional transition metal dichalcogenide with ultra-high energy confinement*, Optics Express **26**(12), 2018, pp. 15819–15824, DOI: 10.1364/OE.26.015819.
[14] SUN F., HE S., *Waveguide bends by optical surface transformations and optic-null media*, Journal of the Optical Society of America B **35**(4), 2018, pp. 944–949, DOI: 10.1364/JOSAB.35.000944.
[15] XU W., ZHU Z.H., LIU K., ZHANG J.F., YUAN X.D., LU Q.S., QIN S.Q., *Toward integrated electrically controllable directional coupling based on dielectric loaded graphene plasmonic waveguide*, Optics Letters **40**(7), 2015, pp. 1603–1606, DOI: 10.1364/OL.40.001603.
[16] QI Z., ZHU Z., XU W., ZHANG J., GUO C., LIU K., YUAN X., QIN S., *Electrically tuneable directional coupling and switching based on multimode interference effect in dielectric loaded graphene plasmon waveguides*, Journal of Optics **18**(6), 2016, article 065003, DOI: 10.1088/2040-8978/18/6/065003.
[17] KANG M., CHONG Y.D., WANG H.-T., ZHU W., PREMARATNE M., *Critical route for coherent perfect absorption in a Fano resonance plasmonic system*, Applied Physics Letters **105**(13), 2014, article 131103, DOI: 10.1063/1.4896972.
[18] HU B., WANG Q.J., ZHANG Y., *Broadly tunable one-way terahertz plasmonic waveguide based on nonreciprocal surface magneto plasmons*, Optics Letters **37**(11), 2012, pp. 1895–1897, DOI: 10.1364/OL.37.001895.
[19] LI W., KUANG D., FAN F., CHANG S., LIN L., *Subwavelength B-shaped metallic hole array terahertz filter with InSb bar as thermally tunable structure*, Applied Optics **51**(29), 2012, pp. 7098–7102, DOI: 10.1364/AO.51.007098.
[20] LIU K., TORKI A., HE S., *One-way surface magnetoplasmon cavity and its application for nonreciprocal devices*, Optics Letters **41**(4), 2016, pp. 800–803, DOI: 10.1364/OL.41.000800.
[21] HU B., WANG Q.J., ZHANG Y., *Slowing down terahertz waves with tunable group velocities in a broad frequency range by surface magneto plasmons*, Optics Express **20**(9), 2012, pp. 10071–10076, DOI: 10.1364/OE.20.010071.
[22] SÁNCHEZ-GIL J., GÓMEZ RIVAS J., *Thermal switching of the scattering coefficients of terahertz surface plasmon polaritons impinging on a finite array of subwavelength grooves on semiconductor surfaces*, Physical Review B **73**(20), 2006, article 205410, DOI: 10.1103/PhysRevB.73.205410.
[23] OSZWAŁDOWSKI M., ZIMPEL M., *Temperature-dependence of intrinsic carrier concentration and density of states effective mass of heavy holes in InSb*, Journal of Physics and Chemistry of Solids **49**(10), 1988, pp. 1179–1185, DOI: 10.1016/0022-3697(88)90173-4.
[24] HOWELLS S.C., SCHLIE L.A., *Transient terahertz reflection spectroscopy of undoped InSb from 0.1 to 1.1 THz*, Applied Physics Letters **69**(4), 1996, pp. 550–, DOI: 10.1063/1.117783.
[25] HALEVI P., RAMOS-MENDIETA F., *Tunable photonic crystals with semiconducting constituents*, Physical Review Letters **85**(9), 2000, pp. 1875–1878, DOI: 10.1103/PhysRevLett.85.1875.
[26] DAI X., XIANG Y., WEN S., HE H., *Thermally tunable and omnidirectional terahertz photonic bandgap in the one-dimensional photonic crystals containing semiconductor InSb*, Journal of Applied Physics **109**(5), 2011, article 053104, DOI: 10.1063/1.3549834.
[27] VAFAPOUR Z., *Slowing down light using terahertz semiconductor metamaterial for dual-band thermally tunable modulator applications*, Applied Optics **57**(4), 2018, pp. 722–729, DOI: 10.1364/AO.57.000722.

[28] Bai Q., Liu C., Chen J., Cheng C., Kang M., Wang H.-T., *Tunable slow light in semiconductor metamaterial in a broad terahertz regime*, Journal of Applied Physics **107**(9), 2010, article 093104, DOI: 10.1063/1.3357291.

[29] Lin X.-S., Huang X.-G., *Tooth-shaped plasmonic waveguide filters with nanometeric sizes*, Optics Letters **33**(23), 2008, pp. 2874–2876, DOI: 10.1364/OL.33.002874.

[30] Palamaru M., Lalanne Ph., *Photonic crystal waveguides: out-of-plane losses and adiabatic modal conversion*, Applied Physics Letters **78**(11), 2001, pp. 1466–1468, DOI: 10.1063/1.1354666.

Received December 31, 2020
in revised form February 19, 2021